ACS APPLIED MATERIALS & INTERFACES

Research Article

Cite This: ACS Appl. Mater. Interfaces 2018, 10, 5269−5277

www.acsami.org

Toward the Development of an Artificial Brain on a Micropatterned and Material-Regulated Biochip by Guiding and Promoting the Differentiation and Neurite Outgrowth of Neural Stem/Progenitor Cells

Yung-Chiang Liu,[†,¶] I-Chi Lee,[*,‡,§,¶] and Kin Fong Lei[*,∥,⊥,#]

[†]Ph.D. Program in Biomedical Engineering, College of Engineering, [‡]Graduate Institute of Biochemical and Biomedical Engineering, [∥]Graduate Institute of Medical Mechatronics, and [⊥]Department of Mechanical Engineering, Chang Gung University, Taoyuan 333, Taiwan

[§]Neurosurgery Department and [#]Department of Radiation Oncology, Chang Gung Memorial Hospital, Linkou, Taoyuan 333, Taiwan

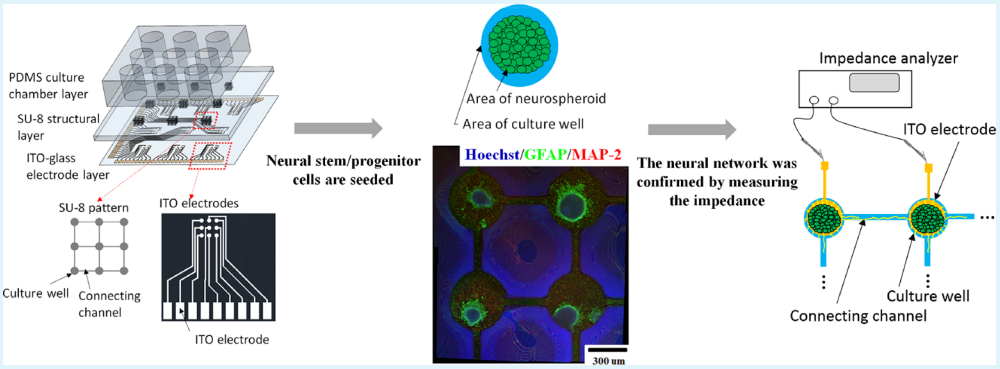

ABSTRACT: An in vitro model mimicking the in vivo environment of the brain must be developed to study neural communication and regeneration and to obtain an understanding of cellular and molecular responses. In this work, a multilayered neural network was successfully constructed on a biochip by guiding and promoting neural stem/progenitor cell differentiation and network formation. The biochip consisted of 3 × 3 arrays of cultured wells connected with channels. Neurospheroids were cultured on polyelectrolyte multilayer (PEM) films in the culture wells. Neurite outgrowth and neural differentiation were guided and promoted by the micropatterns and the PEM films. After 5 days in culture, a 3 × 3 neural network was constructed on the biochip. The function and the connections of the network were evaluated by immunocytochemistry and impedance measurements. Neurons were generated and produced functional and recyclable synaptic vesicles. Moreover, the electrical connections of the neural network were confirmed by measuring the impedance across the neurospheroids. The current work facilitates the development of an artificial brain on a chip for investigations of electrical stimulations and recordings of multilayered neural communication and regeneration.

KEYWORDS: *neural network, biochip, neural stem/progenitor cells, micropatterns, polyelectrolyte multilayer films*

INTRODUCTION

Neural engineering has recently become an attractive area to quantitatively understand how the brain functions and neurons communicate. Most current investigations were designed to record signals transmitted from one neuron to another in animal models.[1−4] For example, electrodes are implanted in the neural tissue of an animal to characterize the complex changes in impedance in response to neural reactions.[1] The advancement of electrode implants has enabled achievements in a number of research areas such as prostheses[5−7] and neuronal diseases.[8,9] These excellent achievements were based on a top-down approach to collect signals from the complicated neural tissue or stimulate the brain. Normally, large numbers of animals and experiments are required to obtain statistically meaningful results. However, an animal model may not be appropriate to study the regeneration of neural networks and the molecular mechanism of neural communication. Thus, an in vitro model is generally adopted to mimic the in vivo environment of the brain. This bottom-up approach is more feasible for regulating cell growth, and the cellular response can be monitored continuously.

Neural stem/progenitor cells (NSPCs) are normally used to develop an in vitro model for investigations of neural communication and regeneration, because they possess the ability to self-renew and differentiate into functional neurons.[10] However, guidance of the direction of neurite outgrowth and

Received: November 23, 2017
Accepted: January 25, 2018
Published: February 5, 2018

DOI: 10.1021/acsami.7b17863
ACS Appl. Mater. Interfaces 2018, 10, 5269−5277

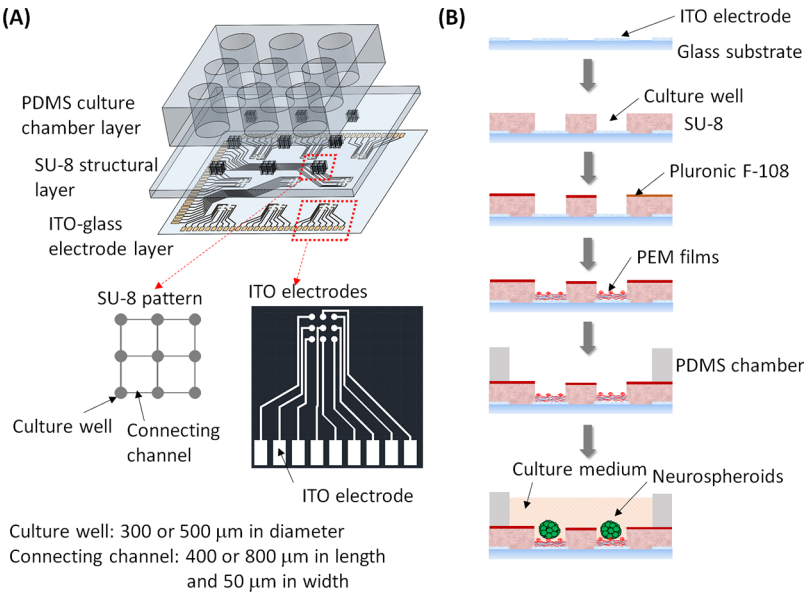

Figure 1. Design and fabrication of the biochip. (A) Schematic illustrating the design of the biochip. (B) Process used to fabricate the biochip.

the differentiation of neurons with synaptic functions is difficult to achieve.[11,12] In the past decade, scientists have reported different approaches for guiding directional neurite outgrowth, such as nerve conduits,[13,14] nanofibrous scaffolds,[15] micropatterns,[16] and guidance molecules.[17] For example, the direction of neurite outgrowth was guided to reconstruct a nervous system using a tubular structure to induce spatial constraints and chemical factors to induce the outgrowth.[13,14] Moreover, the alignment and growth pattern of cells are highly influenced by the dimension of the micropatterned grooves.[18] The topography of the groove/ridge was reported to affect cell behaviors.[19] The use of the micropatterns is generally believed to be the most effective approach to guide the direction of neurite outgrowth.[17,20] On the other hand, numerous methods have been reported to promote the differentiation of functional neurons, such as electrical stimulation,[21] growth factors,[22−24] and polyelectrolyte multilayer (PEM) films.[25,26] These methods modulate cellular responses and direct the differentiation of NSPCs. The use of PEM films is one of the more appropriate approaches for successfully promoting the differentiation of NSPCs into neurons with synaptic functions.[25,26] PEM films are constructed as a multilayer structure assembled by layer-by-layer electrical adsorption of positively and negatively charged materials.[27,28] Because of the use of different preparation conditions, including pH, temperature, and polarity, the properties of PEM films are adjustable for use in various biological applications.[29−32] As shown in our previous study of NSPCs cultured on PEM films without serum and growth factors, the cells are induced to differentiate into functional neurons and a substantial neurite outgrowth is observed.[25] Moreover, NSPC differentiation was further promoted by combining PEM films and an electric field.[26] NSPCs were cultured on PEM films [poly-L-lysine (PLL) and poly-L-glutamic acid (PLGA)] deposited on an indium tin oxide (ITO) surface. A greater number of NPSCs differentiated into functional neurons using this combined approach. The results obtained using these excellent approaches have revealed their abilities to guide the direction of the neurite outgrowth and promote the differentiation of functional neurons. However, few studies have explored the development of in vitro multilayered neural network/artificial brain on chip.

In the current work, a multilayered neural network was successfully constructed on a micropatterned and material-regulated biochip that guided and promoted NSPC differentiation and neurite outgrowth. To validate the connection of the neural network, impedance measurements across neurospheroids were performed to provide quantitative evidence and validate the connections of the neural network. Here, the biochip consisted of nine 3 × 3 arrays of cultured wells connected with channels. PEM films embedded with an ITO electrode were deposited on the bottom surface of the culture wells. Neurospheroids were cultured and developed on the culture wells. The direction of neurite outgrowth was guided by the micropatterns and the differentiation of functional neurons was promoted by the PEM films. After culture, a connected neural network was successfully constructed on the biochip. Moreover, the function and the connections of the neural network were evaluated by immunofluorescence staining and impedance measurements, respectively. The functionality of synapses was also investigated using a synaptic activity assay. On the other hand, the electrical connections of the neural network were confirmed by measuring the impedance across the culture wells. When the neurospheroids were connected through neurites, the impedance was significantly reduced because of the conductivity characteristics of neurites. The current work successfully reports the development of a multilayered neural network on a biochip. Our results facilitate the development of an artificial brain on a chip for investigations of electrical stimulations and recordings of multilayered neural communication and regeneration.

EXPERIMENTAL SECTION

Isolation of Cortical NSPCs. Cerebral cortical NSPCs were isolated from ED14-15 Wistar rat embryos using a previously reported protocol, with modification.[33] The animal experiments performed in this study were conducted in accordance with the recommendations of the Institutional Animal Care and Use Committee at Chang Gung University, Taiwan (IUPAC Permit CGU14-114). Cerebral cortical tissue was collected and suspended in 37 °C Hank's balanced salt solution (HBSS) (5.4 mM KCl, 0.3 mM Na_2HPO_4, 0.4 mM KH_2PO_4,

DOI: 10.1021/acsami.7b17863
ACS Appl. Mater. Interfaces 2018, 10, 5269−5277

4.2 mM $NaHCO_3$, 1.3 mM $CaCl_2$, 0.5 mM $MgCl_2 \cdot 6\ H_2O$, 0.6 mM $MgSO_4 \cdot 7\ H_2O$, 137 mM NaCl, and 5.6 mM D-glucose; the pH was adjusted to 7.4 with NaOH). The tissue was then cut into small pieces and centrifuged at 1000 rpm for 7 min. Cell pellets were isolated from the tissue and washed with warm HBSS. Then, cell pellets were resuspended in Dulbecco's modified Eagle's medium-F12 (12500-062, Gibco, USA) containing the N-2 supplement (17502408, Gibco, USA). Afterward, NSPCs were cultured in T25 flasks (Corning, NY, USA) at 37 °C and 5% CO_2 in a humidified incubator. After 4 days of culture and passage, neurospheroids formed and were suspended in the medium for further experiments.

Design and Fabrication of the Multilayered Neural Network on the Biochip. The biochip was a platform for the construction and evaluation of the multilayered neural network. It consisted of nine 3 × 3 arrays of cultured wells connected with channels. The bottom of each culture well contained an embedded ITO electrode. A schematic illustrating the design of the biochip is shown in Figure 1A. The biochip was constructed from a polydimethylsiloxane (PDMS; Sylgard 184, Dow Corning, USA) culture chamber layer, a SU-8 structural layer, and an ITO-glass electrode layer. The PDMS layer was a 5 mm thick 40 × 40 mm^2 layer containing nine punched holes with an 8 mm in diameter. The ITO-glass substrate was purchased from Uni-Onward Corp., Taiwan, and its surface resistance was 15−18 Ω. The process used to fabricate the biochip is illustrated in Figure 1B. First, the ITO electrodes were fabricated on the ITO-glass substrate using standard photolithography and HCl etching. Then, 100−120 μm thick SU-8 2050 negative photoresist (MicroChem, USA) was coated at 1500 rpm on the ITO-glass substrate and developed based on the pattern of a 3 × 3 array of cultured wells connected with channels. The culture wells and the connecting channels were designed to be 300 and 500 μm in diameter and 400 and 800 μm in length, respectively. The width of the connecting channel was approximately 50 μm. Thus, the SU-8 layer became a structural layer designed to hold the neurospheroids in the culture wells and guide neurite outgrowth in the channels. During photoresist development, the culture wells were aligned with the ITO electrodes under a photomask aligner. Next, the chip was treated with oxygen plasma, and Pluronic F-108 (cat. no.: 542342; Sigma, USA) was applied to the SU-8 surface to prevent the cells and PEM films from binding. Because a difference in height occurs between the SU-8 layer and the non-SU-8 layer, the SU-8 layer was treated with 2.5 mg/mL Pluronic F-108 using a small brush. The chip was placed upside down and treated with a light coating of Pluronic F-108 on the SU-8 layer to prevent the Pluronic F-108 solution from flowing into the non-SU-8 layer. After air drying, PEM coating procedures were performed. PEM films were prepared by alternating physical deposition of 1 mg/mL cationic PLL [molecular weight (MW): 15 000−30 000; Sigma, USA] and 1 mg/mL anionic PLGA (MW: 3000−15 000; Sigma, USA). On the basis of our previous experience, 3.5 layers of PLL/PLGA films were the optimal amount for promoting the differentiation of functional neurons.[25,26] Finally, neurospheroids were seeded on the films and placed in the culture wells using tweezers. The biochip was then transferred to a 37 °C and 5% CO_2 humidified incubator for culture. After 5 days of incubation, multilayered neural networks were observed on the micropatterned and material-regulated biochip.

Lactate Dehydrogenase (LDH) Activity Assay. A cytotoxicity detection kit (cat. no.: 11644793001; Roche, Germany) was used to quantify the release of LDH into the culture medium, which serves as an indicator of cell damage, to investigate the cell viability after 5 days of culture. The medium was collected and incubated with cytotoxicity detection reagents, according to the manufacturer's protocol. The LDH content represented by the optical density was monitored at 490 nm with a reference wavelength of 630 nm using a multimode microplate reader (Synergy HT; BioTek Instruments, USA).

Analysis of the Area Ratio of Neurospheroids on Culture Wells. The area ratio of neurospheroids on culture wells was defined as the percentage of the area of neurospheroids and the area of culture wells to study the growth of neurospheroids cultured on culture wells of different diameters. The area of a neurospheroid was calculated by measuring the diameter of the neurospheroid under a microscope (Leica DM IL, Germany) with a digital camera (CoolSNAP cf, Photometrics, USA). For each data point, at least 10 values were selected for statistical analysis using ImageJ computer software.

Analysis of the Directional Growth and Elongation of Neurites. The directional growth and elongation of neurites were guided and promoted by culturing neurospheroids on the micropatterned and material-regulated biochip. Microscopic images of neurospheroids were captured for analysis after 5 days in culture. The directional growth and elongation of neurites are presented as a radiation plot showing the tips of the neurites. The length of the growing neurites was defined as the direct measurement of the distance from the edge of the neurospheroid to the tip of the neurite, that is, end-to-end distance.

Definition of the Average Connection Ratio of the Neural Network. The connections of the neural network were analyzed from microscopic images. For a 2 × 2 network, four culture wells and four connecting channels were involved. Neurospheroids were cultured in the culture wells, and their neurites were connected through the channels. An average connection ratio of the neural network was defined as the average percentage of neurite outgrowth in each channel.

Immunocytochemistry. For immunocytochemical characterization, the cells that had been cultured on the biochip for 5 days were fixed with 70% methanol for 5−10 min and washed three times with phosphate-buffered saline (PBS). After fixation, cells were incubated overnight with the primary antibody diluted in PBS at 4 °C. A rabbit polyclonal antiglial fibrillary acidic protein (GFAP) antibody (1:500; cat. no.: AB5804; Millipore, USA) was utilized to study cell differentiation into astrocytes. A rabbit monoclonal antimicrotubule associated protein 2 (MAP2) antibody (1:500; cat. no.: MAB3418; Millipore, USA) was utilized to study cell differentiation into neurons. A Hoechst 33342 nucleic acid staining solution (1:2000; cat. no.: H3570; Invitrogen, USA) was used to stain the nucleus. The cells were then incubated with the appropriate secondary antibody for 2 h at room temperature to visualize the signal. A fluorescein isothiocyanate (FITC)-conjugated goat antimouse IgG antibody (1:250; cat. no.: AP181F; Millipore, USA) and FITC-conjugated goat antirabbit IgG antibody (1:250; cat. no.: AP187F; Millipore, USA) were used as the secondary antibodies. Immunostained cells were visualized by indirect fluorescence under a confocal fluorescence microscope (LSM 510 META; Zeiss, Germany).

Labeling of Active Synapses. FM1-43 labeling of functional synapses was performed, according to the manufacturer's protocol. After 5 days in culture, the culture medium was removed. Then, a high potassium HBSS solution (HBSS solution but with 90 mM KCl) containing 2 μM fluorescent styryl membrane probe (FM1-43) lipid dye (cat. no.: F35355; Invitrogen, USA) was added for 60 s to stimulate uptake. Fluorescent images were captured to analyze the functionality of neurons. Afterward, the cells were washed three times in HBSS solution for 5 min to remove the surface-bound FM1-43. The synapses were then destained by incubating cells with a high potassium HBSS solution without the lipid dye for 150 s. A second fluorescent image of each well was captured and compared with the first image to determine the release and turnover of synaptic vesicles.[26] Fluorescent images were captured under a fluorescence microscope at 510 nm.

Impedance Measurements of the Electrical Connections of the Neural Network. An ITO electrode was embedded at the bottom of each well. The electrical connections of two neurospheroids were determined by measuring the impedance across two electrodes. Impedance measurements were conducted using an impedance analyzer (VersaSTAT 4; Princeton Applied Research, USA). A potential of 0.1 V_{rms} was applied across the electrodes, and the impedance data from 1 Hz to 10 kHz were collected for each measurement. On the basis of an analysis of the measurement sensitivity (data not shown), impedance at 1 kHz quantitatively described the linkage of neurites and was used to analyze the electrical connections of the neural network.

Statistical Analysis. Data are expressed as the mean values ± standard deviations from each independent experiment. Each experiment was repeated at least five times. The statistical significance

DOI: 10.1021/acsami.7b17863
ACS Appl. Mater. Interfaces 2018, 10, 5269−5277

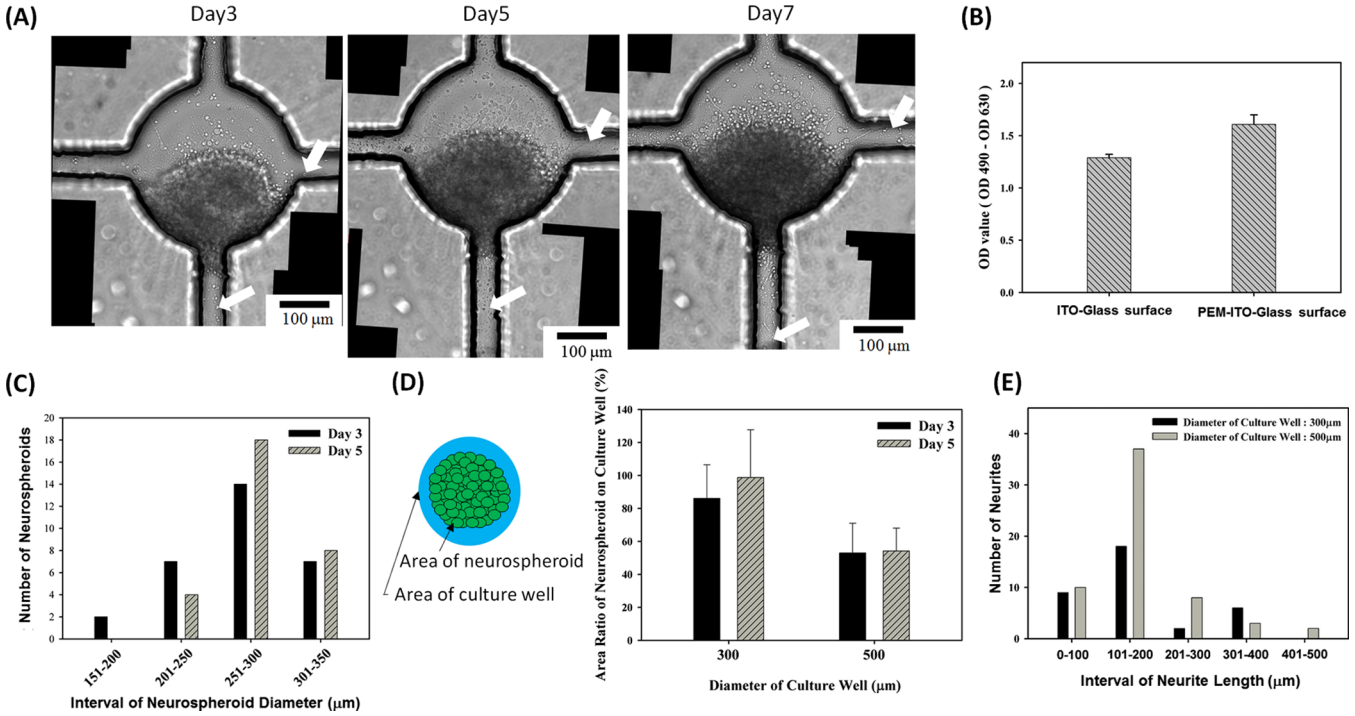

Figure 2. Investigation of the effects of spatial constraints on guiding and promoting neurite outgrowth. (A) Microscopic images show the outgrowth and elongation of neurites along the channels. (B) LDH cytotoxicity analysis of neurospheroids cultured on the ITO-glass and PEM−ITO-glass surfaces. (C) Analysis of the diameters of neurospheroids on days 3 and 5 of culture. (D) Analysis of the area ratio of the neurospheroids on the culture wells on days 3 and 5 of culture. (E) Analysis of the length of neurites that developed from neurospheroids cultured on the 300 and 500 μm culture wells.

between the experimental groups was determined using the *t*-test and indicated as: @ for $p < 0.05$; ## for $p < 0.01$; *** and ### for $p < 0.005$; and ****, ####, and &&&& for $p < 0.001$.

RESULTS AND DISCUSSION

Investigation of the Space Constraints for Guiding and Promoting Neurite Outgrowth. The SU-8 photoresist was used to construct the culture wells and the connecting channels to contain the neurospheroids and guide neurite outgrowth. Here, the thickness of the photoresist was 100−120 μm and a sufficient height was determined to provide spatial constraints. Microscopic images showing the outgrowth and elongation of neurites along the channels are shown in Figure 2A. During the 7 day culture period, neurospheroids were maintained in the culture well and neurite growth was guided along the channels. Moreover, an LDH cytotoxicity analysis was performed to evaluate the cytotoxicity of the PEM films, and the result is shown in Figure 2B. Neurospheroids were cultured on ITO-glass and PEM−ITO-glass surfaces for 5 days. The LDH contents were not significantly different in the cells cultured on the two surfaces. Thus, the PEM films displayed limited cytotoxicity.

The growth of the neurospheroids during the 5 day culture course was investigated on the PEM−ITO-glass surface. Figure 2C shows the analysis of the diameters of neurospheroids from 50 to 350 μm at 50 μm intervals. The result was collected from 30 neurospheroids at 3 and 5 days of culture. The diameter of most neurospheroids ranged from 251 to 300 μm. During culture, small neurospheroids grew and a significant reduction in the number of neurospheroids less than 250 μm in diameter was observed. In contrast, the number of neurospheroids with diameters ranging from 251 to 300 μm was significantly increased. On the basis of this result, neurospheroids grew on the PEM−ITO-glass surface until the diameter reached 251−300 μm. The observation that neurospheroids did not exhibit unlimited growth is reasonable because limited nutrient and gas exchange occur in the center of the neurospheroid.[34] Moreover, the culture wells were designed with two diameters, 300 and 500 μm, to study the correlation between spatial constraints and neurospheroid growth, because the diameters of the neurospheroids ranged from 251 to 300 μm. Neurospheroids were cultured on PEM films deposited in the culture wells. The area ratio of the neurospheroids on the culture wells was analyzed and is shown in Figure 2D. For the 300 μm culture well, the ratio was 70−80% on day 3 and was greater than 90% on day 5. Thus, the neurospheroids and neurites did not have adequate space to grow. On the other hand, the ratio was maintained at 50−60% for the 500 μm culture well during the culture course. More importantly, the outgrowth and elongation of neurites were promoted because sufficient space was available. The analysis of the length of neurites that grew from neurospheroids cultured on the 300 and 500 μm culture wells is shown in Figure 2E. A greater number of and longer neurites (even 401−500 μm) were observed when neurospheroids were cultured on 500 μm culture wells. The total number of neurites increased from 35 to 60 because of the increased diameter of the culture wells. On the basis of these results, the growth space directly influenced the differentiation of neurospheroids. Thus, the design of the micropatterns was critical for guiding the direction of neurite outgrowth and promoting the outgrowth and elongation of the neurites.

Analysis of the Ability of PEM Films to Promote Neurite Outgrowth and Induce the Differentiation of Functional Neurons. The outgrowth and elongation of

DOI: 10.1021/acsami.7b17863
ACS Appl. Mater. Interfaces 2018, 10, 5269−5277

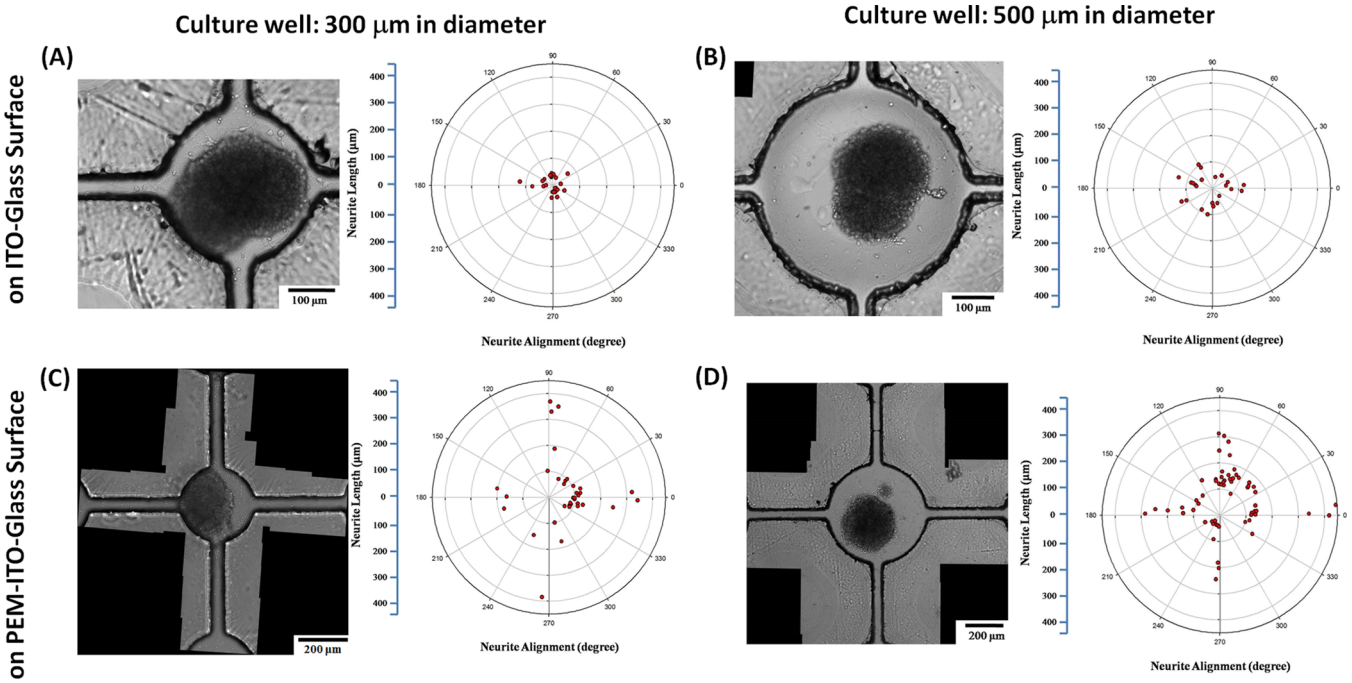

Figure 3. Microscopic images and radiation plots of neurite outgrowth. Neurospheroids were cultured on (A) ITO-glass surface in 300 μm culture wells, (B) ITO-glass surface in 500 μm culture wells, (C) PEM−ITO-glass surface in 300 μm culture wells, and (D) PEM−ITO-glass surface in 500 μm culture wells.

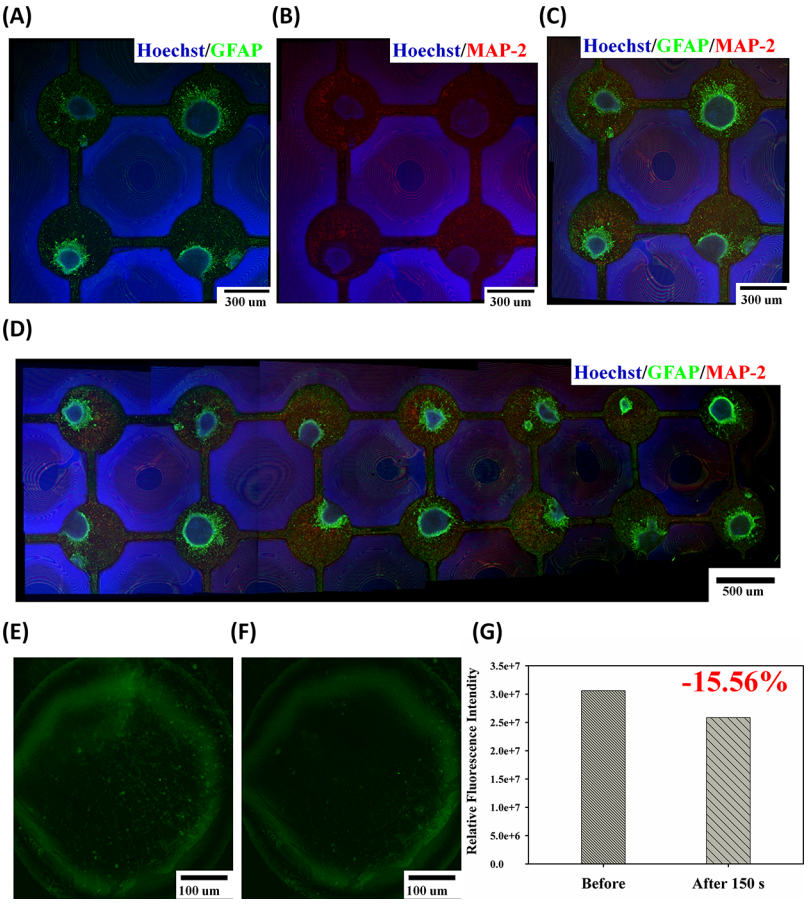

Figure 4. Study of NSPC differentiation. (A−C) Microscopic images of immunofluorescence staining for astrocytes (GFAP), neurons (MAP2), and nuclei (Hoechst 33342). (D) Microscopic image of immunofluorescence staining showing a large-scale neural network. (E,F) Microscopic images showing fluorescent FM1-43 labeling of recycling synaptic vesicles. (G) Quantification of the decrease in the relative fluorescence intensity before and after stimulation.

DOI: 10.1021/acsami.7b17863
ACS Appl. Mater. Interfaces 2018, 10, 5269−5277

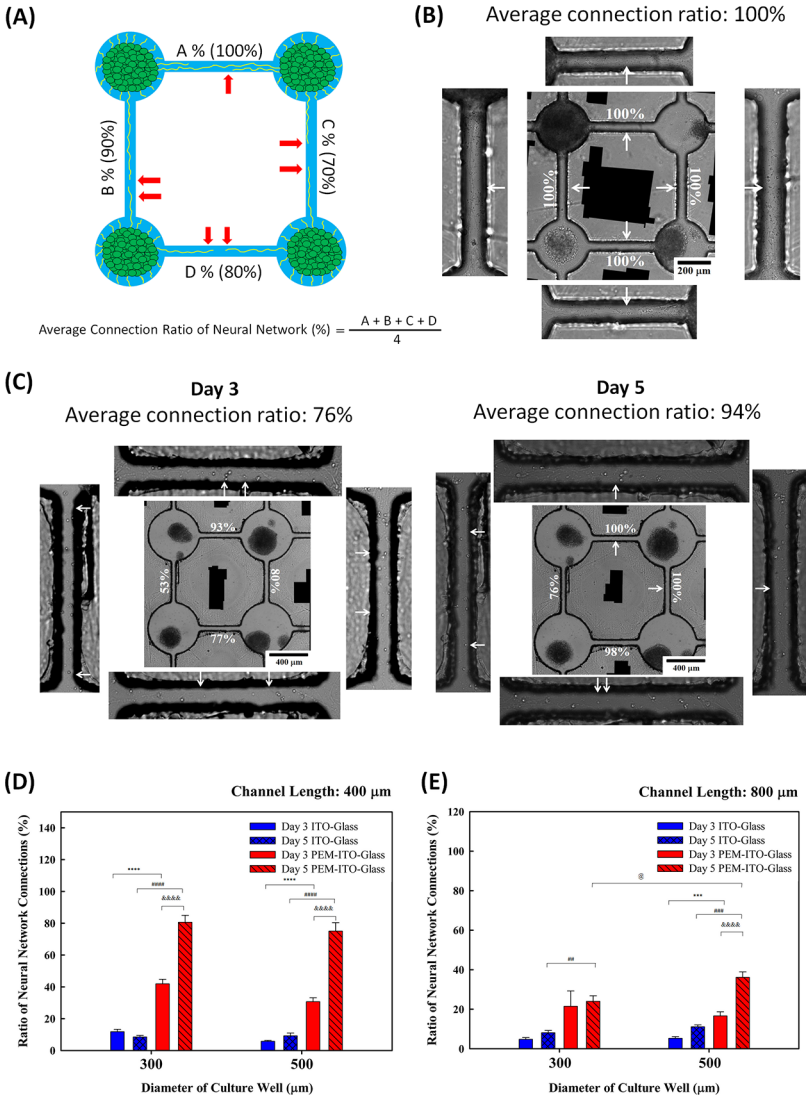

Figure 5. Analysis of the connections of the multilayered neural network. (A) Definition and calculation of the average connection ratio of the neural network. (B) Representative microscopic image of a 100% connected neural network. (C) Microscopic images of a neural network on days 3 and 5 of culture. (D,E) Analysis of the connection ratio under different spatial constraints (300 and 500 μm culture wells) and microenvironmental conditions (ITO-glass and PEM−ITO-glass surfaces). The lengths of connecting channels were (D) 400 and (E) 800 μm.

neurites were also promoted by the PEM films. Neurospheroids were cultured on the 300 and 500 μm culture wells that either contained or lacked the PEM films for 5 days. Microscopic images and radiation plots showing the direction and length of the neurites are shown in Figure 3. Both ITO-glass and PEM−ITO-glass surfaces were suitable for promoting neurospheroid attachment and the neurite outgrowth. However, in wells lacking the PEM films, the longest neurite was approximately 100 μm in the 300 μm culture well (Figure 3A) and 150 μm in the 500 μm culture well (Figure 3B). In contrast, in wells containing the PEM films, the longest neurite was approximately 350 μm in the 300 μm culture well (Figure 3C) and greater than 400 μm in the 500 μm culture well (Figure 3D). Thus, the PEM films promoted the outgrowth and elongation of neurites.

NSPC differentiation was investigated using immunocytochemistry after neurospheroids were cultured on 500 μm culture wells containing the PEM films for 5 days. Immunofluorescence staining for GFAP (green), MAP2 (red), and Hoechst 33342 (blue) was used to identify astrocytes, neurons, and nuclei, respectively. Images of the immunofluorescence staining are shown in Figure 4A−C. NSPCs successfully differentiated into astrocytes and neurons. Our previous study investigated the differentiation of NSPCs cultured on ITO−PEM and ITO-glass with electrical stimulation.[26] NSPCs cultured on $(PLL/PLGA)_n$/ITO-glass and bare ITO-glass with an electrical stimulation of 80 mV produced a high percentage of neurons and displayed long neurites. However, Figure 4 shows a higher expression of GFAP than MAP2. Notably, fluorescence interference occurred in the SU-8 photoresist, particularly red fluorescence (MAP2). The red fluorescence of the laser irradiation intensity was slightly decreased to decrease the interference, which may have resulted in the appearance of a lower MAP2 level in Figure 4. Different wavelengths of fluorescence will be examined in the future to avoid interference. In addition, neurospheroids were connected by astrocytes and neurons along the channels. Moreover, a large scale neural network was constructed and is shown in the images presented in Figure 4D, which were assembled from multiple images of immunofluorescence staining. Fourteen

DOI: 10.1021/acsami.7b17863
ACS Appl. Mater. Interfaces 2018, 10, 5269−5277

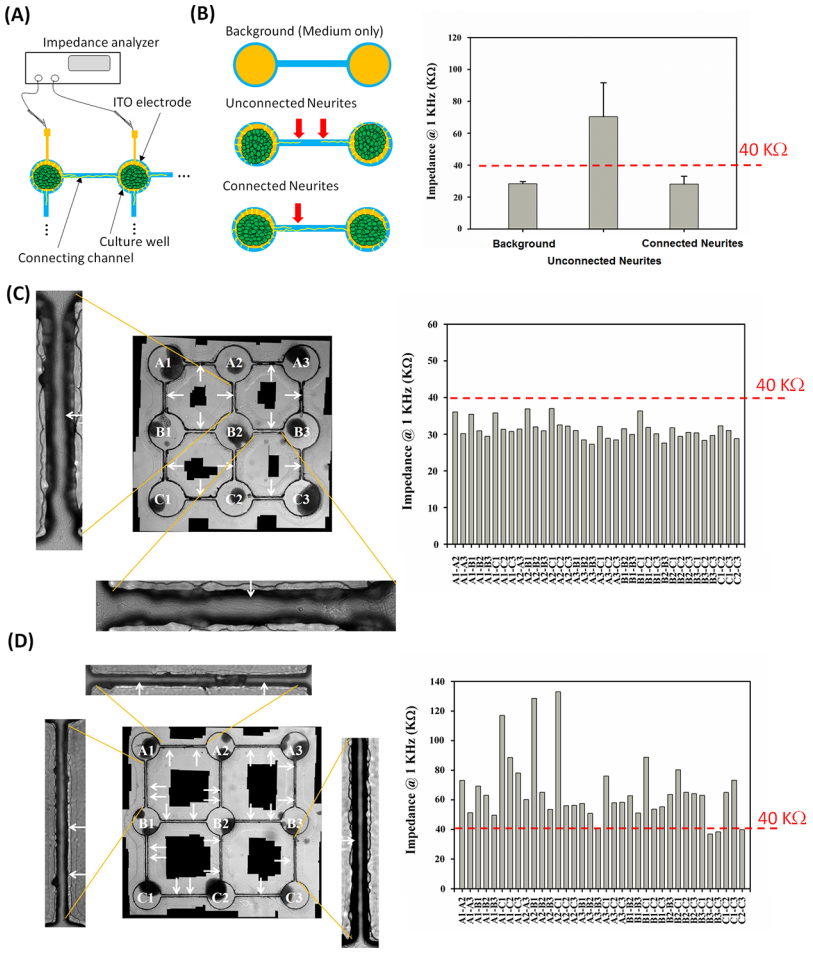

Figure 6. Analysis of the electrical connections of the multilayered neural network. (A) Schematic illustrating the experimental setup. (B) Impedance values for the background (medium only), unconnected neurites, and connected neurites across two electrodes. (C) Microscopic images of a 100% connected 3 × 3 neural network and the impedance values observed for each pair electrodes. (D) Microscopic images of a partially connected neural network and the impedance values observed for each pair of electrodes.

neurospheroids were connected by astrocytes and neurons along the channels. The layers of the neural network were well-defined by the micropatterns. Furthermore, the functionality of the synapses and activity-dependent vesicle cycling were evaluated using FM1-43 lipid dye in the synaptic activity assay. The membranes of synaptic vesicles were stained with FM1-43 lipid dye following stimulation with a high potassium solution for 60 s. If stained vesicles undergo exocytosis in a dye-free medium, FM1-43 molecules dissociate from the membrane because of the concentration gradient and the fluorescence decreases after the second stimulation with the high potassium solution without lipid dye. Figure 4E shows the presence of green fluorescence at the location of synaptic vesicles. The concentration of synaptic vesicle protein at synapses in the neurons was observed, and the result revealed the development of mature neurons. Then, the fluorescence intensity was decreased after the second stimulation with a high potassium solution lacking the lipid dye for 150 s, as shown in Figure 4F. The quantitative analysis of the fluorescence intensity before and after stimulation is shown in Figure 4G. A 15.56% decrease was observed, and the result indicated that the synaptic vesicles were functional and recyclable.

Investigation of the Connections of the Multilayered Neural Network. The connections of a 2 × 2 neural network were studied by determining the average connection ratio. The definition and calculation are shown in Figure 5A. A representative image of a 100% connected neural network is shown in Figure 5B. The neurites that developed from four neurospheroids were connected along the channels. Figure 5C shows the microscopic images of a neural network on days 3 and 5 of culture. Progressive development of the neural network was observed, and the average connection ratio ranged from 76 to 94%. Therefore, the average connection ratio was used to evaluate the effect of the space constraints and the microenvironment on network formation. The formation of neural networks was studied under different spatial constraints (300 and 500 μm culture wells) and microenvironmental conditions (ITO-glass and PEM−ITO-glass surfaces). The results obtained for the channel length of 400 μm are shown in Figure 5D. Obviously, a higher connection ratio was obtained when neurospheroids were grown on the PEM films. The connection ratio observed on day 5 was significantly increased compared with day 3 and was approximately 80%. Because the channel length was 400 μm, the network was relatively easily connected in the presence of the PEM films. Thus, no statistically significant difference was observed between 300 and 500 μm culture wells. However, for the channel length of 800 μm, the connection ratio on day 5 was significantly increased when neurospheroids were cultured on 500 μm culture wells deposited with the PEM films, as shown in Figure 5E. This

DOI: 10.1021/acsami.7b17863
ACS Appl. Mater. Interfaces 2018, 10, 5269−5277

finding further confirmed that longer neurites developed when more space was provided. Because individual differences in neurospheroids may affect neurite outgrowth, different sides of the pattern have different connection ratios. In addition, a space is available for neurosphere attachment and a gap is present between the edge of the sphere and the connection channel. The spheroid size and the attachment position may affect the distance and the neurite connection speed. The ability to collect data from multiple sites might increase the representation of the connection data and the statistical results may help to present the significance. The connections of a 2 × 2 neural network were studied based on the average connection ratios of four sides, and the ratio data shown in Figure 5D,E were derived from 10 individual 2 × 2 neural networks (five individual 2 × 2 neural networks for the TCPS group). Furthermore, neurite outgrowth was more stable after 5 days of culture than after 3 days culture; the error between largest and smallest connection ratios was obviously decreased after 5 days of culture (data not shown).

Although microscopic imaging is conventionally used to analyze neural connections, the function of the neural connections cannot be validated using this technique. Electrical connections of the network must be measured to examine neural communication. Here, an impedance analysis was applied to measure the impedance values between neurospheroids. The experimental setup is shown in Figure 6A. Because cell membranes are electrically insulated, impedance measurements have been used to analyze cellular responses.[35−37] The impedance values of background (medium only), unconnected neurites, and connected neurites were measured and are shown in Figure 6B. A significant difference was observed between unconnected and connected neurites. When the neurospheroids attached on the ITO electrodes without connecting neurites, the effective electrode surface area was reduced and led to an increase of the impedance value across the electrodes. In contrast, when the neurospheroids were connected by neurites, electrical connections were constructed and the impedance value across the electrodes was significantly reduced. A threshold of 40 kΩ was defined to determine the electrical connections of the neurospheroids. Figure 6C shows a 100% connected 3 × 3 neural network. The impedance values between every pair of electrodes were less than 40 kΩ. The electrical connections of the entire multilayered neural network were confirmed. Moreover, a 3 × 3 neural network with partial connections is shown in Figure 6D. The impedance values across each pair of electrodes were also measured. Most of the impedance values were greater than 40 kΩ, indicating that these neurites were not connected. Although the connected neurites in the channels were observed in the microscopic image, the impedance analysis provided further evidence for the electrical connections of the neural network.

CONCLUSIONS

Multilayered neural networks were constructed on a micropatterned and material-regulated biochip, as evidenced by the differentiation and development of NSPCs. Spatial constraints and microenvironmental conditions were investigated for their abilities to guide and promote neurite outgrowth. NSPCs differentiation and synaptic function were investigated using immunocytochemistry. Impedance measurements were conducted across two neurospheroids to provide quantitative evidence and validate the connections of the neural network. The current in vitro model represents a platform that mimics the brain in vivo and is a feasible tool for studies of cellular and molecular responses. Neural communication and regeneration were investigated using not only immunocytochemistry but also electrical stimulations and recordings. This approach paves the way toward the development of an artificial brain on a chip for various disease models, for example, neurological disorders and Parkinson's disease.

AUTHOR INFORMATION

Corresponding Authors

*E-mail: iclee@mail.cgu.edu.tw. Phone: +886-3-2118800 ext. 5985 (I.-C.L.).

*E-mail: kflei@mail.cgu.edu.tw. +886-3-2118800 ext. 5345 (K.F.L.).

ORCID

I-Chi Lee: 0000-0001-6527-0077

Kin Fong Lei: 0000-0002-5356-2221

Author Contributions

¶Y.-C.L. and I.-C.L. contributed equally to this work.

Notes

The authors declare no competing financial interest.

ACKNOWLEDGMENTS

The authors acknowledge the financial supports from the Ministry of Science and Technology, Taiwan (project no.: MOST105-2221-E-182-017) and Chang Gung Memorial Hospital, Linkou, Taiwan (projects no.: CMRPD1G0221-2, BMRPC49, and BMRPC05).

REFERENCES

(1) Williams, J. C.; Hippensteel, J. A.; Dilgen, J.; Shain, W.; Kipke, D. R. Complex Impedance Spectroscopy for Monitoring Tissue Responses to Inserted Neural Implants. *J. Neural. Eng.* **2007**, *4*, 410−423.

(2) Nisbet, D. R.; Pattanawong, S.; Ritchie, N. E.; Shen, W.; Finkelstein, D. I.; Horne, M. K.; Forsythe, J. S. Interaction of Embryonic Cortical Neurons on Nanofibrous Scaffolds for Neural Tissue Engineering. *J. Neural. Eng.* **2007**, *4*, 35.

(3) Jackson, A.; Mavoori, J.; Fetz, E. E. Long-term Motor Cortex Plasticity Induced by an Electronic Neural Implant. *Nature* **2006**, *444*, 56−60.

(4) Nuyujukian, P.; Kao, J. C.; Fan, J. M.; Stavisky, S. D.; Ryu, S. I.; Shenoy, K. V. Performance Sustaining Intracortical Neural Prostheses. *J. Neural. Eng.* **2014**, *11*, 066003.

(5) Dhillon, G. S.; Horch, K. W. Direct Neural Sensory Feedback and Control of a Prosthetic Arm. *IEEE Trans. Neural Syst. Rehabil. Eng.* **2005**, *13*, 468−472.

(6) Normann, R. A.; Maynard, E. M.; Rousche, P. J.; Warren, D. J. A Neural Interface for a Cortical Vision Prosthesis. *Vision Res.* **1999**, *39*, 2577−2587.

(7) Guggenmos, D. J.; Azin, M.; Barbay, S.; Mahnken, J. D.; Dunham, C.; Mohseni, P.; Nudo, R. J. Restoration of Function After Brain Damage Using a Neural Prosthesis. *Proc. Natl. Acad. Sci. U.S.A.* **2013**, *110*, 21177−21182.

(8) Clarke, D. J.; Brundin, P.; Strecker, R. E.; Nilsson, O. G.; Björklund, A.; Lindvall, O. Human Fetal Dopamine Neurons Grafted in a Rat Model of Parkinson's Disease: Ultrastructural Evidence for Synapse Formation Using Tyrosine Hydroxylase Immunocytochemistry. *Exp. Brain Res.* **1988**, *73*, 115−126.

(9) Freeman, T. B.; Cicchetti, F.; Hauser, R. A.; Deacon, T. W.; Li, X.-J.; Hersch, S. M.; Nauert, G. M.; Sanberg, P. R.; Kordower, J. H.; Saporta, S.; Isacson, O. Transplanted Fetal Striatum in Huntington's Disease: Phenotypic Development and Lack of Pathology. *Proc. Natl. Acad. Sci. U.S.A.* **2000**, *97*, 13877−13882.

DOI: 10.1021/acsami.7b17863
ACS Appl. Mater. Interfaces 2018, 10, 5269−5277

(10) Azari, H.; Osborne, G. W.; Yasuda, T.; Golmohammadi, M. G.; Rahman, M.; Deleyrolle, L. P.; Esfandiari, E.; Adams, D. J.; Scheffler, B.; Steindler, D. A.; Reynolds, B. A. Purification of Immature Neuronal Cells from Neural Stem Cell Progeny. *PLoS One* **2011**, *6*, No. e20941.
(11) Gage, F. H. Mammalian Neural Stem Cells. *Science* **2000**, *287*, 1433−1438.
(12) Tam, R. Y.; Fuehrmann, T.; Mitrousis, N.; Shoichet, M. S. Regenerative Therapies for Central Nervous System Diseases: a Biomaterials Approach. *Neuropsychopharmacology* **2013**, *39*, 169−188.
(13) Jenkins, P. M.; Laughter, M. R.; Lee, D. J.; Lee, Y. M.; Freed, C. R.; Park, D. A Nerve Guidance Conduit with Topographical and Biochemical Cues: Potential Application Using Human Neural Stem Cells. *Nanoscale Res. Lett.* **2015**, *10*, 972.
(14) Yucel, D.; Kose, G. T.; Hasirci, V. Polyester Based Nerve Guidance Conduit Design. *Biomaterials* **2010**, *31*, 1596−1603.
(15) Hackelberg, S.; Tuck, S. J.; He, L.; Rastogi, A.; White, C.; Liu, L.; Prieskorn, D. M.; Miller, R. J.; Chan, C.; Loomis, B. R.; Corey, J. M.; Miller, J. M.; Duncan, R. K. Nanofibrous Scaffolds for the Guidance of Stem Cell-Derived Neurons for Auditory Nerve Regeneration. *PLoS One* **2017**, *12*, No. e0180427.
(16) Nyberg, T.; Shimada, A.; Torimitsu, K. Ion Conducting Polymer Microelectrodes for Interfacing with Neural Networks. *J. Neurosci. Methods* **2007**, *160*, 16−25.
(17) Eichmann, A.; Le Noble, F.; Autiero, M.; Carmeliet, P. Guidance of Vascular and Neural Network Formation. *Curr. Opin. Neurobiol.* **2005**, *15*, 108−115.
(18) Craighead, H. G.; James, C. D.; Turner, A. M. P. Chemical and Topographical Patterning for Directed Cell Attachment. *Curr. Opin. Solid State Mater. Sci.* **2001**, *5*, 177−184.
(19) Curtis, A.; Wilkinson, C. Topographical Control of Cells. *Biomaterials* **1997**, *18*, 1573−1583.
(20) Lu, Y.-P.; Yang, C.-H.; Yeh, J. A.; Ho, F. H.; Ou, Y.-C.; Chen, C. H.; Lin, M.-Y.; Huang, K.-S. Guidance of Neural Regeneration on the Biomimetic Nanostructured Matrix. *Int. J. Pharm.* **2014**, *463*, 177−183.
(21) Al-Majed, A. A.; Neumann, C. M.; Brushart, T. M.; Gordon, T. Brief Electrical Stimulation Promotes the Speed and Accuracy of Motor Axonal Regeneration. *J. Neurosci.* **2000**, *20*, 2602−2608.
(22) Savignat, M.; Vodouhe, C.; Ackermann, A.; Haikel, Y.; Lavalle, P.; Libersa, P. Evaluation of Early Nerve Regeneration Using a Polymeric Membrane Functionalized With Nerve Growth Factor (NGF) After a Crush Lesion of the Rat Mental Nerve. *J. Oral Surg.* **2008**, *66*, 711−717.
(23) Petersen, P. H.; Zou, K.; Hwang, J. K.; Jan, Y. N.; Zhong, W. Progenitor Cell Maintenance Requires Numb and Numblike During Mouse Neurogenesis. *Nature* **2002**, *419*, 929−934.
(24) Johe, K. K.; Hazel, T. G.; Muller, T.; Dugich-Djordjevic, M. M.; McKay, R. D. Single Factors Direct the Differentiation of Stem Cells From the Fetal and Adult Central Nervous System. *Genes Dev.* **1996**, *10*, 3129−3140.
(25) Lee, I.-C.; Wu, Y.-C. Facilitating Neural Stem/Progenitor Cell Niche Calibration for Neural Lineage Differentiation by Polyelectrolyte Multilayer Films. *Colloids Surf., B* **2014**, *121*, 54−65.
(26) Lei, K. F.; Lee, I.-C.; Liu, Y.-C.; Wu, Y.-C. Successful Differentiation of Neural Stem/Progenitor Cells Cultured on Electrically Adjustable Indium Tin Oxide (ITO) Surface. *Langmuir* **2014**, *30*, 14241−14249.
(27) Decher, G. Fuzzy Nanoassemblies: Toward Layered Polymeric Multicomposites. *Science* **1997**, *277*, 1232−1237.
(28) Tsai, H.-A.; Wu, R.-R.; Lee, I.-C.; Chang, H.-Y.; Shen, C.-N.; Chang, Y.-C. Selection, Enrichment, and Maintenance of Self-Renewal Liver Stem/Progenitor Cells Utilizing Polypeptide Polyelectrolyte Multilayer Films. *Biomacromolecules* **2010**, *11*, 994−1001.
(29) Mulchandani, A.; Trojanowicz, M. Analytical Applications of Planar Bilayer Lipid Membranes. *Anal. Bioanal. Chem.* **2004**, *379*, 347−350.
(30) Shiratori, S. S.; Rubner, M. F. pH-Dependent Thickness Behavior of Sequentially Adsorbed Layers of Weak Polyelectrolytes. *Macromolecules* **2000**, *33*, 4213−4219.
(31) Kučerka, N.; Tristram-Nagle, S.; Nagle, J. F. Structure of Fully Hydrated Fluid Phase Lipid Bilayers with Monounsaturated Chains. *J. Membr. Biol.* **2006**, *208*, 193−202.
(32) Wu, G.; Zhang, X. Unconventional Layer-By-Layer Assembly for Functional Organic Thin Films. In *Polymer Thin Films*; Hashim, A. A., Ed.; InTech, 2010; pp 143−160.
(33) Wang, J.-H.; Hung, C.-H.; Young, T.-H. Proliferation and Differentiation of Neural Stem Cells on Lysine−Alanine Sequential Polymer Substrates. *Biomaterials* **2006**, *27*, 3441−3450.
(34) Persano, L.; Rampazzo, E.; Basso, G.; Viola, G. Glioblastoma Cancer Stem Cells: Role of the Microenvironment and Therapeutic Targeting. *Biochem. Pharmacol.* **2013**, *85*, 612−622.
(35) Liu, L.; Xiao, X.; Lei, K. F.; Huang, C.-H. Quantitative Impedimetric Monitoring of Cell Migration Under the Stimulation of Cytokine or Anti-Cancer Drug in a Microfluidic Chip. *Biomicrofluidics* **2015**, *9*, 034109.
(36) Lei, K. F.; Tseng, H.-P.; Lee, C.-Y.; Tsang, N.-M. Quantitative Study of Cell Invasion Process under Extracellular Stimulation of Cytokine in a Microfluidic Device. *Sci. Rep.* **2016**, *6*, 25557.
(37) Lei, K. F.; Lin, B.-Y.; Tsang, N.-M. Real-time and Label-Free Impedimetric Analysis of the Formation and Drug Testing of Tumor Spheroids Formed via the Liquid Overlay Technique. *RSC Adv.* **2017**, *7*, 13939−13946.

DOI: 10.1021/acsami.7b17863
ACS Appl. Mater. Interfaces 2018, 10, 5269−5277